Laser Surface Modification of Tool Steel for Semi-Solid Steel Forming

Dermot Brabazon, Sumsun Naher and Patrick Biggs

Materials Processing Research Centre, Dublin City University, Glasnevin, Dublin 9, Ireland

Abstract.

This paper presents an analysis of the effect of CO_2 laser processing parameters on the surface modification and heat treatment of steels. The CO_2 laser and sample movement process parameters are presented. The controlled operation of these in conjunction with each other is required to obtain better surface hardness and structure. H13 tool steel samples were rotated at high speeds to keep exposure times below 0.3s. Laser processed samples were analysed using EDX spectroscopy, optical microscopy, Vickers and Martens micro-hardness testing, and X-ray diffraction (XRD). Results show how the hardness profile through the surface is related to the laser treatment and resultant microstructures. Increased surface hardness was noted due to a complete microstructural transformation to an amorphous state in the glazed samples. The usefulness of such coatings on tool steels, in conjunction with other thermal barriers, for the forming of semi-solid steel alloys is presented.

Keywords: glazing, semi-solid forming, surface heat treatment, thermal barrier coating.

Introduction

Much work has been performed over the last decade investigating possibilities for the semi-solid forming of high temperature melting metals including Ni, Ti, Cu and Fe based alloys [1-8]. Forming of these materials in the semi-solid state could give the usual advantages we expect from semi-solid forming, including increased fluidity, near net shape formability and higher part density and strength. Using as low a temperature as possible, compared with liquid casting, is more energy efficient at these high temperatures. Barriers to the large scale semi-solid forming of these alloys includes the lack of knowledge of their rheology, the lack of sufficiently durable tooling and the requirement for determination of process procedure [9]. For repeatable high speed mass production of high quality parts with this process, new die materials and forms need to be developed. Many workers have investigated various die materials and forms that could be used for this purpose [1021]. Die materials investigated include iron based high temperature tool steel, H13, molybdenum based, TMZ, tungsten based, Anviloy, and nickel based alloy, Inconel. Surface treatments are often used to improve the strength of surface and subsurface layers of hot-working dies in order to mitigate against the damages due to both thermal and mechanical stress. This holds back the nucleation and propagation of heat checking and prolongs the service life of hot working dies. Ceramic coating materials that have been applied to these tools include Al_2O_3, ZrO_2, $ZrSiO_4$, $MgAl_2O_3$, Y_2ZrO_5, WC, and Si_3N_4. Techniques for the application of these coatings include thin coating techniques such as PVC and CVD, as well as thicker coating techniques such as thermal spraying, brazing, explosive welding, laser melt injection and the use of bulk ceramic inserts [19-26].

H13 (wt%: 5.5Cr, 1.8Mo, 1.2V, 1.2Si, 0.5Mn, 0.45C, 0.3Ni, bal. Fe) is a common popular die steel for high temperature usage. High temperature oxidation resistance is a basic requirement which is a characteristic of this material. Other steel dies including PVD coated ledeburitic cold working steels have been investigated in the past for semi-solid steel forming [17]. Laser glazing is a surface treatment process that forms an amorphous layer by causing rapid heating followed by quick quenching. This amorphous structure is hard, wear-resistant, oxidation-resistant and corrosion resistant. Once the surface of the steel becomes amorphous its thermal conductivity can reduce by a factor of ten [27, 28]. Amorphous materials are also considerably harder and more corrosion resistant than their crystalline counterparts [29-31]. This increased hardness and corrosion resistance coupled with the reduced thermal conductivity present the laser glazing process as a technique that can be used to allow the development of high temperature tooling. In this technique, the metal substrate tooling would be first glazed to act as a bond coat for a ceramic thermal barrier coating which would be subsequently applied. The work presented here is focused on the development of a technique to achieve surface glazing and to assess the effect of laser processing parameters on the type of surface structures developed and associated mechanical properties.

Materials and Methods

H13 rods of 10mm diameter and 100 mm long were rotated at high speed and passed longitudinally under a continuous CO_2 generated laser beam of 0.2 mm spot diameter. The laser beam thus traced out a spiral laser path on the cylindrical surfaces. The laser power was altered between 825 and 1050 W, the traverse speed between700 and 1200 mm/s and the beam overlap between each helix was set to 30%. An argon assist gas was used to avoid oxidation. The irradiance and exposure times were set as shown in Table 1. The sample rotational speeds and linear traverse speeds were controlled to provide the overlap and the exposure time settings. Exposure times were calculated in the conventional manner by dividing the diameter of the spot size by the point speed. The exposure times and irradiances required were determined from similar previous work [32-34].

Energy Dispersive X-ray Spectroscopy (EDX). The composition of the alloy was check with an Energy Dispersive X-ray spectroscopy system (IMIX PGT X-ray Microanalysis) which was used in conjunction with a Leo 440 Scanning Electron Microscope.

Micro-Hardness. Vickers and Martens micro-hardness readings were recorded. A Leitz 301 was used to measure the Vickers micro-hardness. The Martens micro-hardness was measured with an instrumented FISCHERSCOPE® HM2000 in accordance with ISO 14577.

Table 1 Experimental settings used for the laser surface heat treatment experiments and Martens Hardness and indentation depth results indicated in the last two columns.

Expt. No.	Irradiance (W/m^2)	Exposure Time (ms)	HM	hmax
1	478	0.29	2430	3.29
2	334	0.29	4847	2.29
3	382	0.29	2373	3.32
4	310	0.29	4998	1.99
5	287	0.29	4765	2.3
6	263	0.29	4802	2.01
7	334	0.25	2814	3.19
8	310	0.25	4754	2.23
9	287	0.25	4958	2.01

Expt. No.	Irradiance (W/m^2)	Exposure Time (ms)	HM	hmax
10	263	0. 25	4765	2.31
11	334	0. 21	2036	3.61
12	310	0.21	3946	2.54
13	287	0.21	4191	2.5
14	263	0.21	2464	3.3
15	334	0.17	4077	2.5
16	310	0.17	4767	2.3
17	287	0.17	4357	2.4
18	263	0.17	5738	2.1

Metallography. The rods were sectioned 10 mm from the end of the processed region and prepared for metallographic examination in order to examine the through thickness microstructures. Nital with 2-5% nitric acid and methanol was used for etching. The samples were treated with this etchant for up to 15 seconds which was then washed off. A Leica MF2 Universal optical inverted light microscope was used to take the micrographs.

X-ray Diffraction (XRD). The laser treated specimens were investigated with X-ray diffraction using CuKα radiation in order to find out the extent of transformation to an amorphous structure after laser treatment. The X-ray diffraction pattern was recorded using a Bruker X-ray DIFFRAC^{plus} D8 ADVANCE diffractometer. The pattern was recorded between a 2θ range of 5–35° at 30 kV and 20 mA. A scanning speed of 1 °/min and a chart speed of 5 mm/min were used.

Results

Energy Dispersive X-ray Spectroscopy (EDX). The composition found from EDX for this tool steel was 5.36Cr, 1.59Mo, 1.0Si, 1.0V, 0.49Mn, 0.45C, 0.22Mg, bal. Fe which is the expected composition for a H13 tool steel.

Micro-Hardness. The Martins (HM) hardness and the maximum indentation depths are shown in Table 1. The Vickers hardness measurements, not shown, produced the same trends as the HM values. Sample one and three were processed at a much higher power compared with the other samples. It is believed that the lower hardness readings at the surface of these samples was due to the presence of a ferritic structure resulting from slower cooling which it turn was caused by the greater power density used. This was confirmed also from metallography. The other samples were processed at a powder density of 262, 287, 310, or 334 W/m2 and an exposure time of 0.17, 0.21, 0.25 or 0.29 seconds. All of these latter samples showed a large increase in hardness, up to two times greater, than that of the substrate.

Metallography. The micrographs from the through surface cross section of samples 3, 9, 10 and 17 are shown in Fig. 1.

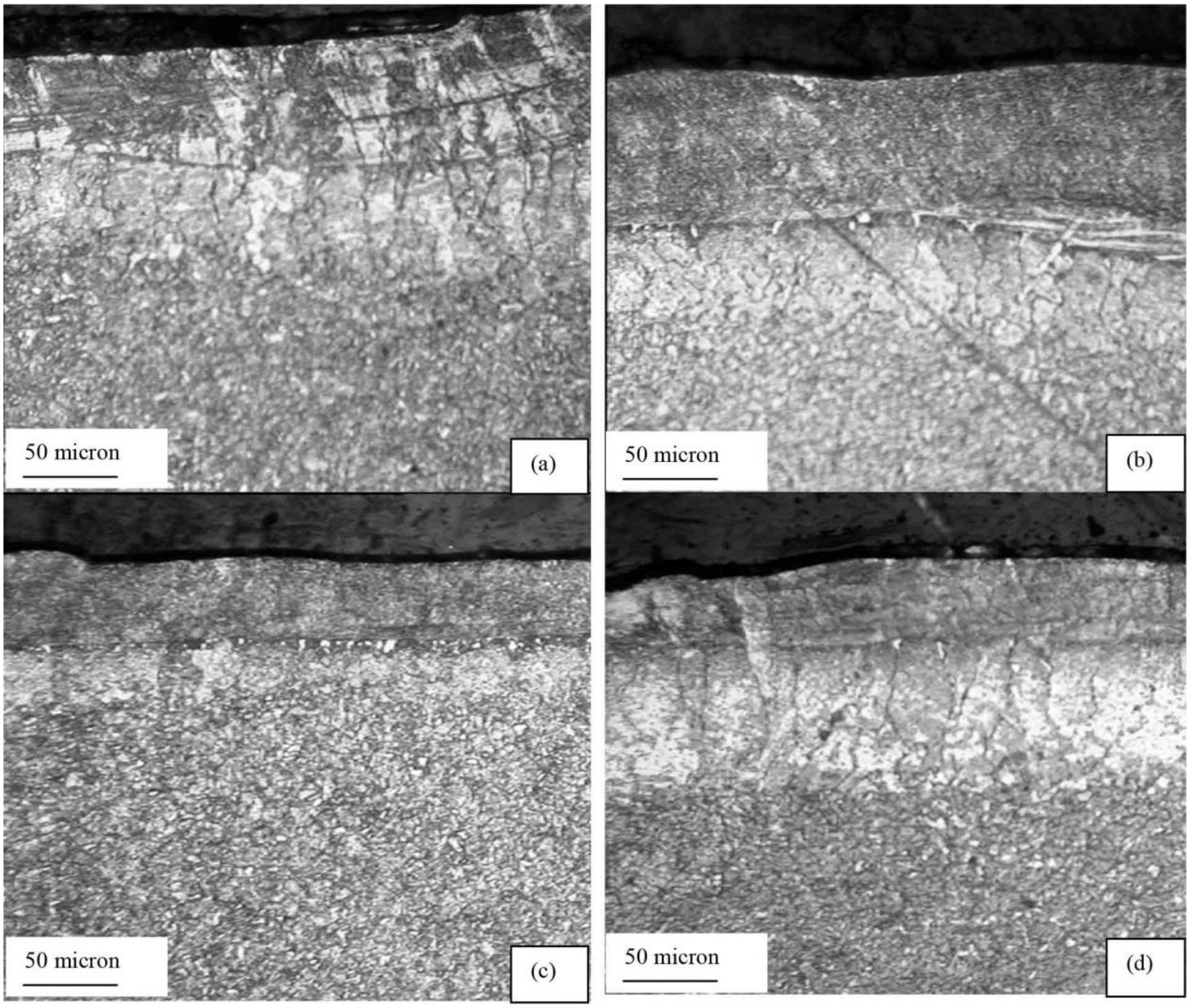

Figure 1 Micrographs of laser surface treated H13 tool steel
(a) sample 3, (b) sample 9, (c) sample 10 and (d) sample 17.

A typical surface microstructure affected depth of 150 µm was noted however this varied depending of the processing conditions. Samples 3, 9 and 17 had an affected region of approximately 150 µm deep, whereas sample 10 showed an affected region 60 µm deep. Like most steel H13 is allotropic which is a reversible phenomenon by which the steel can exist in more than one structure. Fully ferritic structure is obtained only when the carbon content is low. Ferrite is a soft low-strength phase and of body centered cubic crystal structure. The formation of martensite, which is not an equilibrium phase in steel, depends on chemical composition and cooling rate from the high temperature austenite region. Carbon content markedly influences the nature of the formed body centered tetragonal martensite microstructure. In Fig. 1 (a), (b) and (c) where higher heat affected zone was observed, more ferritic structure is seen due to the diffusion of interstitial carbon from unstable martensite structure. EDX showed carbon build up on the sample surface and at the interface between the layer structures. It is important to note also that in order to obtain a glassy structure; the metal must be cooled at a rate such that the nose of the timetemperature transition diagram is avoided. The location of the ferrite phase was different depending on the sample. For sample 3, the ferrite was observed on the surface whereas for samples 9, 10 and 17 it is located approximately 40 µm beneath the surface. Samples 9, 10 and 17 showed some amorphous surface structure as shown by the XRD, see next section. This was achieved with processing conditions which would have brought the surface temperature just above the melt temperature such that very rapid cooling could occur at the fast moving surface. Subsequent to this, reaming heat would slowly be conducted away trough the sample giving the entrapped directionally solidified ferrite grain structure observed

X-ray diffraction (XRD). The X-ray diffraction patterns of H13 tool steel substrate and laser treated specimen 9 surface are shown in Fig. 2.

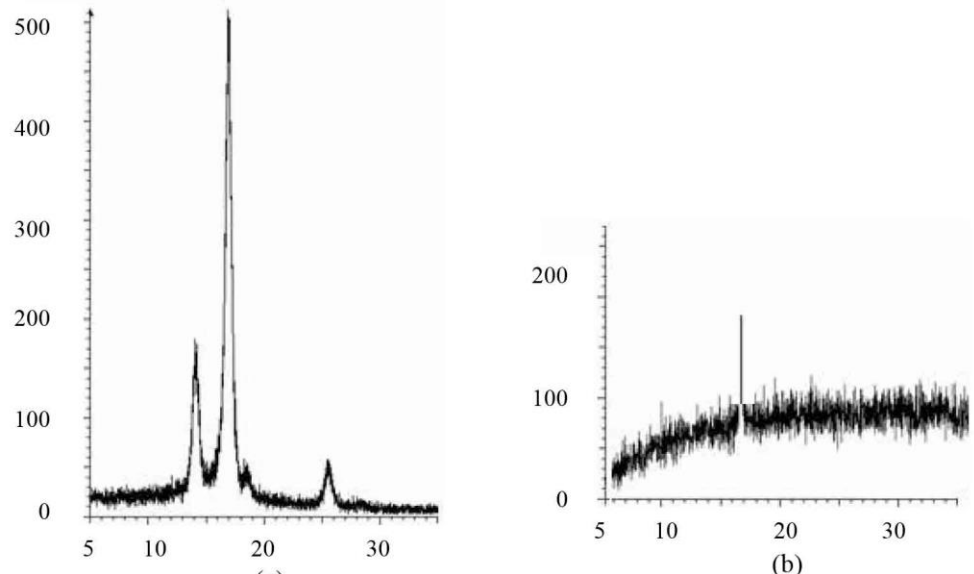

(a)

(b)

Figure 2 X-ray diffraction patterns of counts versus 2θ for H13 tool steel (a) substrate and (b) laser treated specimen surface.

Recorded values for the H13 XRD patterns from the substrate are listed in Table 2. For the substrate three peaks are evident at 14, 17 and 25.5 degree angles with an intensity of 161, 492 and 49 counts respectively. In comparison, the laser treated surface response has only one peak with very low intensity of less than 180 counts. This peak also shifted slightly to the left which could be related to the generation of internal stress due to the laser treatment.

Table 2 Values for H13 tool steel substrate XRD pattern.

Angle (2θ)	d-value	Intensity (Counts)	Intensity (%)
14.050	6.29811	161	32.7
16.888	5.24570	492	100
25.548	3.48382	49	10

Discussion

An advantage of surface glazing is the potential ability of this process to tailor a thermal shock barrier for the underlying die surface [28]. The peaks in Fig. 2 (a) indicate that the X-ray beam has been diffracted by the substrate crystal structure. The broad spectra in Fig. 2 (b) represents the spectra one would expect from an amorphous solid or liquid, characterised by an almost complete lack of periodicity [35]. Laser glazing would be only one part of the potential solution to finding long life tooling. Knowledge gained from thermal barrier coatings (TBC) used for turbine blades is a useful guide to providing a solution to tooling that can withstand similar high temperatures in semi-solid metal processing. Lower total linear thermal expansion which has been noted for glass metals at high temperatures could also enable better functional grading of the TBC [36]. The coating process could follow the steps of laser glazing on the surface of tool steel, followed by thermal spraying a ceramic TBC and followed in turn by laser scanning on the ceramic surface to achieve closed pores and a smoother surface. The metal glazing in this case could either take the place of or be used along with the metal bond layer that is conventionally used for TBCs in aviation applications. Keeping the tooling temperature at an elevated level during processing could also help increase the die life [21]. With continuous operation of the die forming machine, any extra energy used to keep the tool temperature at a high level may be compensated for by the extra die life. Impurities added to the H13 steel that interfere with the diffusion-controlled transformation process such as TiC, CrC or rare earth elements would allow for lower cooling rates to obtain a glass structure and provide a wider potential processing range [35]. Fe base bulk glass metal sheets are already commercially available and are superformable above the glass transition temperature [3739]. After thermal spraying a ceramic coating onto this, it could then be used as a die insert or cladding. Due to the severer requirement for a thermal barrier at these high temperatures, a thicker thermal spraying should be better than either thin PVD or CVD coatings. The extra small amount of porosity in the thermally sprayed coating would be advantageous in the sense that it would increase the degree of insulation. Even with a thicker thermal spray coating, a high temperature thermal barrier coating wash could also be required between each injection [40, 41].

Acknowledgements.

The authors would like to acknowledge the technical support from Martin Johnson and Michael May in performing this study. The authors would also like to acknowledge the EU Cost Action 541 and partners involved therein for providing the opportunity for discussions on this work.

References

[1] H. Bramann, M. Fehlbier, P.R. Sahm and A. Bührig-Polaczek, J. of Mat. Proc. Tech. 155–156 (2004) 1357–1364

[2] D.I. Uhlenhaut, J. Kradolfer, W. Puttgen, J.F. Loffler and P.J. Uggowitzer, Act. Mat. 54 (2006) 2727–2734

[3] M. S. Lewandowski and R.A. Overfelt, Acta mater. Vol. 47, No. 18, (1999) 4695-4710

[4] B.A. Behrens, B. Haller and D. Fischer, Steel Research International, Verlag, 2004

[5] M.Z. Omar, E.J. Palmiere, A.A. Howe, H.V. Atkinson and P. Kapranos, Mat. Sci. and Eng. A 395 (2005) 53–61

[6] R. Kopp, J. Kallweit, T. Moller and I. Seidl, J. of Mat. Proc. Tech. 130–131 (2002) 562–568

[7] Y.Q. Zhao, W.L. Wu and H. Chang, Materials Science and Engineering A 416 (2006) 181–186

[8] M. Ramadan, M. Takita, H. Nomura and N. El-Bagoury, Mat. Sci. and Eng. A430 (2006) 285

[9] http://www.cost541.ulg.ac.be/; accessed 20/05/2008.

[10] J. She and T. Ohji, J. Am. Ceram. Soc., 85, 8 (2002).

[11] S. Meyer-Rau and R. Telle, J. of European Ceramic Society, 25 (2005).

[12] H. Evans, M. Taylor, J. Aerospace Engineering, IMechE, 220, Part G (2006).

[13] V. Velay, G. Bernhart, D. Delagnes and L. Penazzi, Fatigue Fract Engng Struct, 28 (2005).

[14] D.H. Kim, B.M. Kim and C.G. Kang, Int. J. Adv. Manuf. Technol. 27 (2005) 33–39.

[15] K. Das and T.K. Bandyopadhyay, Materials Science and Engineering A379 (2004)

[16] K. Bobzin, E. Lugscheider, M. Maes and P. Immich, 9th Int. Conference on Semi-Solid Processing, Pusan, South Korea, Sept. 2006, Solid State Phenomena, 116-117 (2006) 704-707

[17] G. Hirt, F. Knauf, K. Bobzin and P. Immich, AIP Conf. Proc., Vol. 907 (2007) 1173-1178

[18] P. Cezard, R. Bigot, E. Becker, S. Mathieu, J.C. Pierret and A. Rassili, AIP Conference Proceedings, Vol. 907 Issue 1 (2007) 1155-1160

[19] S. Munstermann and R. Telle, Mat. – wiss, u. Werkstofftech, 37, 4 (2006).

[20] S.Y. Shan, J.F. Yang, J.Q. Gao, W.H. Zhang, and Z.H. Jin, J. Am. Ceram. Soc., 88, 9 (2005) 2594–2596

[21] D. T. Peters, J. G. Cowie, E. F. Brush and S. P. Midson, Die Casting – Toward the Future, NADCA, 30th Sept. – 2nd Oct. 2002., Rosemont, Illinois, USA.

[22] Cladding by shrink fitting, Patent US3664411 (1973)

[23] Multiple layer ceramic tooling, Patent EP1042803 (2000)

[24] Mould insert used as cladding , Patent WO2006004713 (2006)

[25] S. Ettaqi, L. Langlois and R. Bigot, Surface & Coatings Technology 202 (2008) 3306–3315

[26] A. Nascimento, V. Ocelík, M.C. Ierardi, and J. Hosson, Surf. & Coat. Tech. 202 (2008) 2113

[27] Y. Zjang, W.H. Wang and D.A.L. Greer, Nature Materials Letters, Vol. 5 (2006) 857-860.

[28] K. Wang, T. Fujita, W. Chen, T. Nieh, H. Okada, K. Koyama, W. Zhang and A. Inoue, App. Phys. Letters, 2007, Vol. 91

[29] M.F. Ashby and A.L. Greer, Scripta Materialia 54 (2006) 321–326

[30] R.J. DiMelfi, P.G. Sanders, B. Hunter, J.A. Eastman, K.J. Sawley, K.H. Leong and J.M. Kramer, Surface and Coatings Technology, 106 (1998) 30–43

[31] D. Matthews, V. Ocelik, J.De Hosson, Mat. Sci. and Eng. A471 (2007) 155–164

[32] Y. Yang, Y. Song, W. Wu, M. Wang, Thin Solid Films, 1998, Vol. 323, pp. 199-202. [33] W. Jiang, W. Molian, P. Molian, Surf. & Coat. Tech, 2001, Vol. 135, pp. 139-149.

[34] J. Ready, LIA Handbook of Laser Material Processing, Magnolia Publishing, Orlando, 2001.

[35] B.D. Cullity, Elements of X-ray diffraction, 2nd Ed, 1978, ISBN 0-201-01174-3.

[36] H. Kato, H.S. Chen and A. Inoue, Scripta Materialia 58 (2008) 1106–1109

[37] B. Yao, K. Zhang, H. Tan and Y. Li, Journal of Non-Crystalline Solids 354 (2008) 970–974

[38] C.Y. Luo, Y.H. Zhao, X.K. Xi, G. Wang, D.Q. Zhao, M.X. Pan, W.H. Wang and S.Z. Kou, Journal of Non-Crystalline Solids 352 (2006) 185–188

[39] A. Makino, T. Kubota, M. Makabe, C. Chang, A. Inoue, Mat. Sci. and Eng. B148 (2008) 166

[40] Protective barriers in ceramic moulds, Patent WO97/0709 (1999)

[41] Glass powder lubricant for open die forging, Patent US4788842 (1988)